ELSEVIER

Thermochimica Acta 304/305 (1997) 283–290

thermochimica acta

Modulated differential scanning calorimetry: Investigation at structural phase transitions

K.-P. Bohn[a], A. Prahm[a], J. Petersson[b], J.K. Krüger[a,*]

[a] *Fachbereich 10.2, Experimentalphysik, Universität des Saarlandes, Bau, 38, Postfach 151150, 66041 Saarbrücken, Germany*
[b] *Fachbereich 10.3, Technische Physik, Universität des Saarlandes, Bau, 38, Postfach 151150, 66041 Saarbrücken, Germany*

Received 8 August 1996; accepted 12 December 1996

Abstract

Modulated DSC was used to investigate the specific heat around ferroelectric phase transitions. This method has been extended to investigations of slow relaxations within the time domain. For this purpose a suitable cooling assembly is proposed working with liquid nitrogen as well as with liquid helium as a coolant. © 1997 Elsevier Science B.V.

Keywords: Modulated differential scanning calorimetry; Structural phase transitions

1. Introduction

The technique of differential scanning calorimetry (DSC) [e.g. [1,2]] was recently extended by the operation mode of modulated temperature. Reading et al. [3] developed a method superimposing a sinusoidal temperature modulation to a linear temperature change $dT/dt = \text{const}$ commonly used in conventional DSC. Choosing appropriate values for the free adjustable parameters rate $\beta = dT/dt$, amplitude A_T and frequency f_m of the temperature modulation, modulated DSC provides an increased sensitivity in comparison to conventional DSC without loss of resolution [4,5]. In addition to this, modulated DSC allows a direct determination of the specific heat capacity c_p [6]. The possibility to measure c_p even under quasi-isothermal conditions ($\beta = 0$) [7] makes this technique suitable especially for investigations of structural phase transition.

The target of this paper is to show the usefulness of modulated DSC as a rather simple method to investigate caloric properties around structural phase transitions. We will present results for three different ferroelectrics: (i) lead germanate ($Pb_5Ge_3O_{11}$) has been chosen as an example which shows an extremely weak coupling between the order parameter and the thermal properties of the material, (ii) betaine arsenate ($(CH_3)_3NCH_2COO{\cdot}H_3AsO_4$) was chosen to demonstrate the possibility to make modulated DSC measurements at least until 100 K, (iii) triglycinesulfate ($(NH_2CH_2COOH)_3{\cdot}H_2SO_4$, TGS) was chosen to demonstrate the potential of modulated DSC to be used within time domain studies, providing thus information on slow kinetic phenomena which may even appear in the vicinity of 2nd order structural phase transitions.

2. Experimental

For usual DSC and modulated DSC measurements we have used experimental parameters as proposed by

*Corresponding author.

PII S0040-6031(97)00025-7

the manufacturer of the calorimeter. The mathematical algorithm to calculate the specific heat capacity c_p requires a sinusoidal temperature modulation. In order to avoid asymmetric deviations from the sinusoidal temperature modulation we used small modulation amplitudes, small temperature rates and a modulation period of 60 s. The influence of thermal conductivity was further minimized by using only thin plate-like samples. The calibration of the baseline was performed in the same temperature range as the following c_p measurement using the same temperature rate. The heat capacity constant K_{c_p} of the calorimeter was calibrated using sapphire as a standard. In addition to the same temperature range and the same rate β we used the same values for the modulation period P_m and the modulation amplitude A_T as in the case of the following c_p measurement of the sample.

2.1. The cooling unit

For our caloric investigations we have used the TA Instruments Thermal Analyst 2920 MDSC™. The temperature modulation mode of this equipment requires a permanent cooling even at ambient and higher temperatures, the amount of cooling being dependent not only on the temperature range or cooling rate but also on the temperature amplitude A_T and the modulation frequency f_m.

Detailed investigations of relaxation processes in the time domain like the previous reported studies of hypersonic relaxations in the glass transition region of the atactic polymer polyvinylacetate [8,9] generally are time consuming and may take weeks. Modulated DSC measurements in the time domain (TDM-DSC) therefore require an undisturbed permanent cooling during the entire experiment. Therefore, we have modified the standard liquid nitrogen cooling assembly of the TA calorimeter with respect to Fig. 1: a pumping station (P) generates an appropriate under pressure by which the liquid nitrogen is pumped from a Dewar flask (D) via a vacuum isolated transfer tube (T) to the vacuum isolated heat exchanger (H) where it is vaporised. The connection between the heat exchanger and the transfer tube is sealed by an o-ring. The amount of cooling can be adjusted by a needle valve (NV) and checked by a flow meter (FM). This new cooling system allows the operation of the dewar at atmospheric pressure. The Dewar flask can therefore be refilled during measurement without any thermal disturbance of the experiment. The modified cooling system thus allows calorimetric investigations by modulated DSC without any temporal limitations.

Although there are cooling losses (mainly caused by the open design of the DSC set-up) temperatures down to ~110 K could be achieved with N_2 as a cooling gas. As a result of introducing the new cooling assembly, liquid helium can also be used as a coolant. In this way, we were able to realise 63 K at the oven of the calorimeter; moreover, the measurement capabilities of the calorimeter are limited by the measurement and control properties of the calorimeter rather than by the cooling facilities.

The vacuum isolation of the transfer line and the heat exchanger significantly reduce the consumption of the coolant. At 120 K, only ~1.5 l liquid N_2 per hour was needed to perform TDM-DSC measurements.

2.2. TDM-DSC

The DSC cell was usually purged with dry helium gas at a flow rate of 30 ml/min. TDM-DSC measurements of the specific heat capacity of TGS were performed using a temperature modulation with a period $P_m = 60$ s. The amplitude was chosen to be as small as $A_T = 0.2$ K, in order to minimise the temperature range for the mathematical procedure of calculating and averaging the c_p data [7]. Starting at a given mean temperature T_j, we performed a temperature step $\Delta T = T_{j+1} - T_j$. The specific heat capacity $c_p^i(T_{j+1})$, obtained as soon as the new temperature T_{j+1} is reached will be denoted as the instantaneous specific heat capacity response. The relaxed response obtained after a suitable measurement time yields the equilibrium response denoted as $c_p^\infty(T_{j+1})$. The temperature steps ΔT were selected according to the physical requirements.

3. Results and discussion

3.1. Lead germanate

Lead germanate is an uniaxial ferroelectric, exhibiting strong effect on dielectric constant at the ferroelectric phase-transition temperature $T_c = 450.15$ K [10–12], but nearly no effect on the thermal properties.

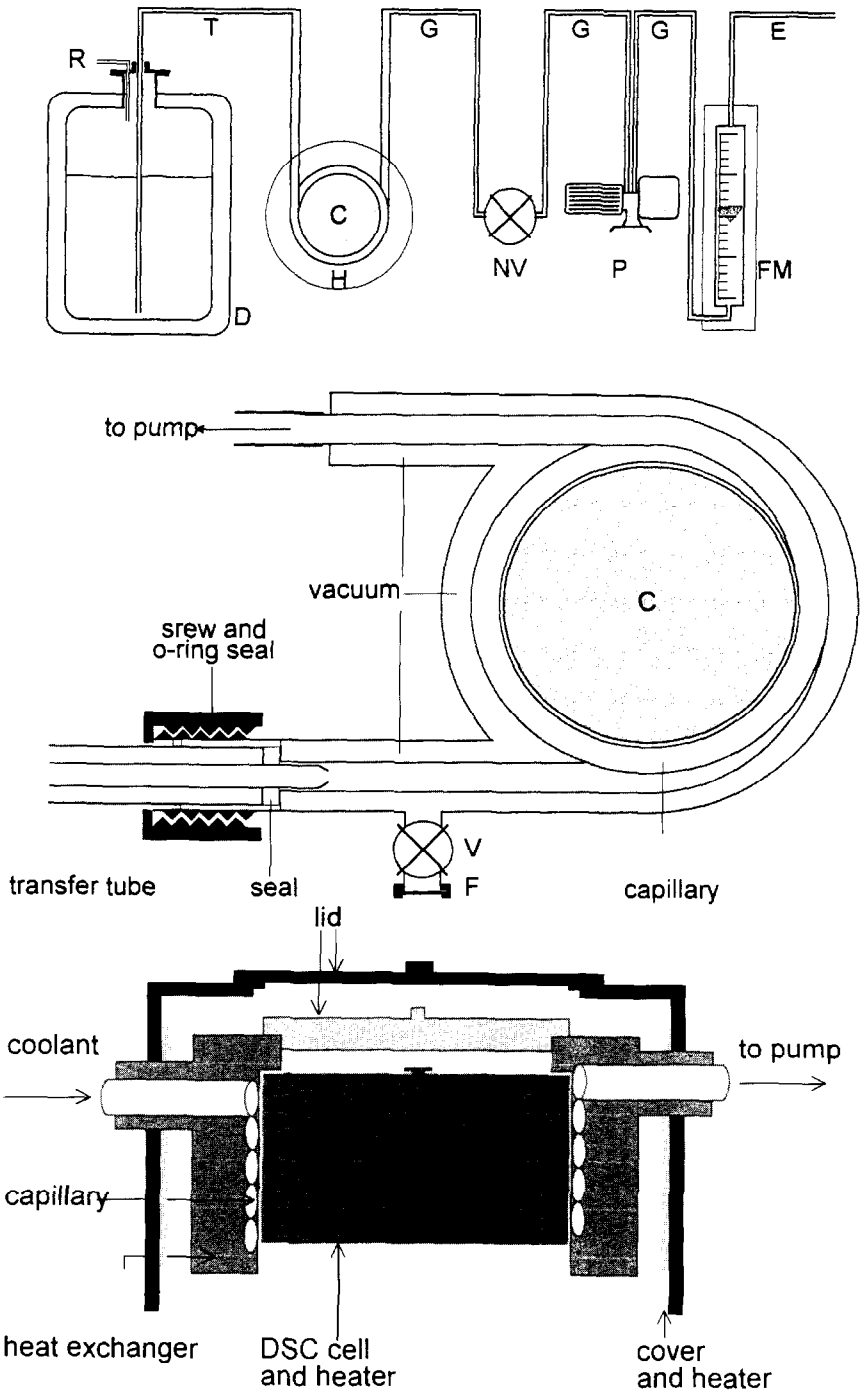

Fig. 1. (a) Schematic set-up of the modified cooling system: D: dewar; R: refill; T: transfer tube; H: heat exchanger; C: oven and DSC cell; G: teflon tubes; V: valve; P: pumping station; FM: flow meter; E: exhaust. (b) Schematic drawing of the heat exchanger. V: valve, F: joining flange to vacuum pump.

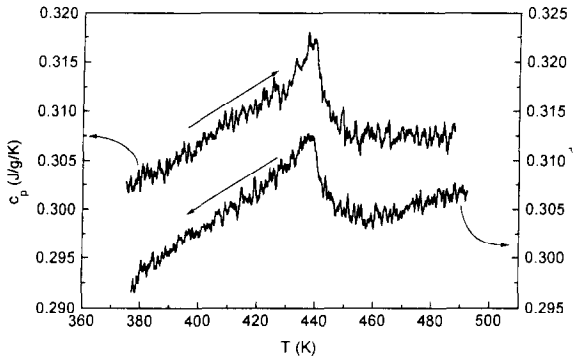

Fig. 2. Specific heat capacity c_p of lead germanate as a function of temperature on heating and cooling. T_c: ferroelectric phase-transition temperature. Sample mass m =18.79 mg; A_T=0.2 K; P_m=60 s and β=0.5 K/min.

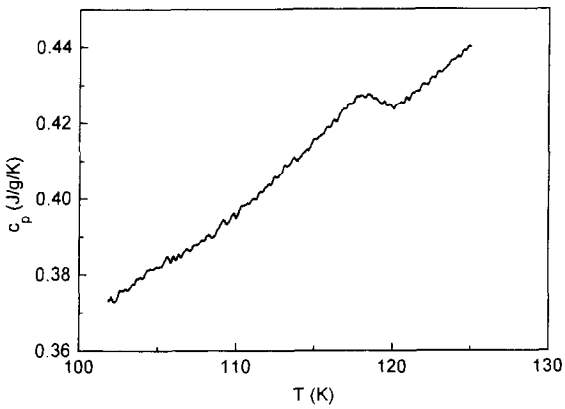

Fig. 3. Specific heat capacity c_p of betaine arsenate as a function of temperature. T_c: ferroelectric phase-transition temperature (119 K). Sample mass m = 16.82 mg; A_T = 0.2 K; P_m = 60 s; and β = 0.15 K/min.

The transition is a weak 1st order transformation. To our knowledge there exist no $c_p(T)$ data in literature illustrating the ferroelectric transition.

Using the new cooling system, Fig. 2 demonstrates the high sensitivity and the high resolution of the calorimeter in the modulation mode. According to the specific heat data (Fig. 2), we find a transition temperature of $T_c = 447.1$ K which is in good agreement with data from literature [10–12]. The transition entropy amounts to 8×10^{-4} Jg^{-1} K^{-1}.

3.2. Betaine arsenate

Betaine arsenate ($(CH_3)_3NCH_2COO{\cdot}H_3AsO_4$) has a paraelectric phase with monoclinic structure at room temperature. At $T_c = 119$ K, it undergoes a phase transition of 2nd order, to a ferroelectric low-temperature phase [13]. This phase transition which significantly affects the dielectric behaviour, resulting in the highest value for the dielectric constant [14] of 10^6, only shows small effects on the thermal properties around the phase transition. Calorimetric investigations of Frühauf et al. [15], performed with an adiabatic calorimeter, revealed a transition entropy $\Delta S = 2.5 \times 10^{-3}$ Jg^{-1} K^{-1}. This result is, by a factor of about eight, larger than that of Klöpperpieper et al. ($\Delta S = 3 \times 10^{-4}$ Jg^{-1} K^{-1}) [13] which was determined from much more sensitive dielectric data. Fig. 3 shows the heat capacity of betaine arsenate as measured by modulated DSC in the range between 100 and 130 K. In accordance with the results of Ref. [13], our $c_p(T)$-curve yields a transition temperature of $T_c = 119$ K and deviates from that of Ref. [15] by −4 K. The transition entropy amounts to $\Delta S = 4 \times 10^{-4}$ Jg^{-1} K^{-1}, which is close to the value of Ref. [13] but deviates significantly from the value given by Ref. [15]. This discrepancy between the modulated DSC data and those obtained with the much more time-consuming and experimentally lavish adiabatic calorimetry is not clear yet, but might be due to differences in crystal quality. The latter argument seems to be supported by the differences in the Curie temperatures. In particular, the modulated DSC results show the efficiency of the new cooling assembly.

3.3. Triglycinesulphate

Triglycinesulphate ($(NH_2CH_2COOH)_3{\cdot}H_2SO_4$, TGS) undergoes a structural phase transition of second order at $T_c = 322.57$ K from a paraelectric high-temperature phase to a ferroelectric low-temperature phase [16], both phases having the monoclinic space groups $P2_1/m$ and $P2_1$, respectively. This phase transition is a prototypic ferroelectric transition and its electrical behaviour has been investigated in great detail (e.g. [17–19]). Special interest also has been paid to the caloric behaviour of TGS and its relation to the ferroelectric order parameter, the spontaneous polarisation P_s [20]. Pioneering work in this field was done by Strukov et al., using ac-calorimetry [16,21,22].

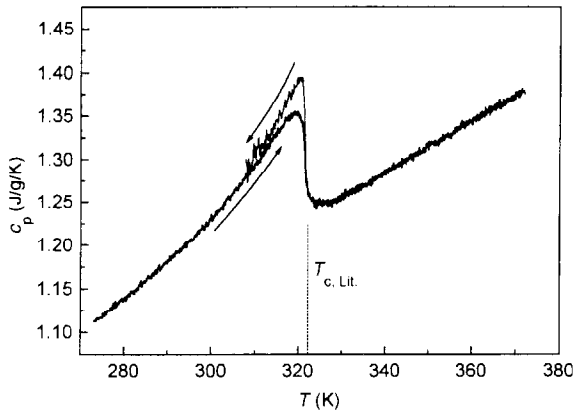

Fig. 4. Specific heat capacity c_p of TGS as a function of temperature, measured on heating and cooling. Heating and cooling rate $\beta = 0.5$ K/min; sample mass m = 17.60 mg; $A_T = 0.2$ K; and $P_m = 60$ s. No defined boundary conditions were realised.

The specific heat capacity data of TGS, as found in the literature, vary significantly between different publications. This holds true for the noncritical (lattice) part of the specific heat as well as for the critical contribution. Deviations up to 20% are typical and are mainly due to impurities and related domain pinning, but as will be seen below, may also be attributed to floating electrical boundary conditions within the ferroelectric state.

Domain-pinning effects on the specific heat, as measured by modulated DSC, are shown in Fig. 4. The modulated DSC measurement were performed on a virgin TGS first heated up to 370 K and then measured on cooling with floating electrical boundary conditions ($\beta = -0.5$ K/min, $P_m = 60$ s and $A_T = 0.2$ K). Subsequently, the measurements were repeated with $\beta = 0.5$ K/min, fixing the other experimental parameters. Both curves reflect nicely the agreement with literature data measured with much more complicated and time-consuming calorimetric techniques. As expected, for a phase transition of second order the transition temperatures T_c of both temperature runs are identical; this holds true for the c_p data of the paraelectric, as well as for the ferroelectric phase well below T_c. The different influence of heating vs. cooling measurements on the specific heat capacity anomaly of TGS has already been reported by Gavrilova et al. [23]. They explain it on the basis of impurities in the crystal that lock the order parameter P_s and, therefore, suppress the evolution of the order-parameter contribution to the specific heat at $T \leq T_c$. Annealing the sample well above T_c greatly increases the mobility of these defects. This results in enhanced defect diffusion which decreases the domain-locking probability and as a result yields a larger anomalous contribution to the heat capacity during a subsequent cooling run. Taraskin et al. [16] found a clear cut correlation between the peak height in the vicinity of T_c, and the annealing time at 363 K.

The full contribution of the ferroelectric ordering to the caloric properties is expected for mono-domain crystal at zero electric field ($E = 0$). Unfortunately, the mono-domain state is hardly realised in a DSC calorimeter; on the other hand, the electrical boundary condition $E = 0$ is experimentally easily realised by covering the sample with a thin gold coating. Fig. 5 (curve a) shows the results of such a measurement ($\beta = 0.2$ K/min, $P_m = 60$s and $A_T = 0.2$ K). The anomalous contribution to $c_p(T)$ exceeds 0.2 J g^{-1} K^{-1} which is close to precision measurements of Strukov et al. [21]. Again, the transition temperature T_c is accurately reproduced.

Since TGS shows a nearly ideal phase transition of second order, we can use a Landau-type theory to describe the critical behaviour and to compare the

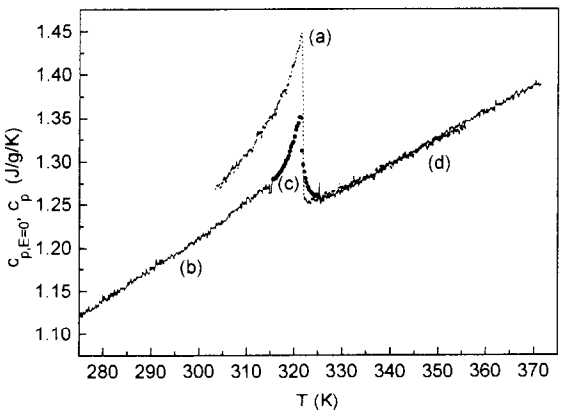

Fig. 5. (a) Measurement of $c_{p,E=0}(T)$ of a gold-sputtered TGS-sample ($m = 20.51$mg) realises boundary condition $E = 0$; heating measurement with heating rate $\beta = 0.2$ K/min, temperature modulation amplitude $A_T = 0.2$ K and modulation period $P_m = 60$ s. (b) and (d) $c_p(T)$ with undefined boundary condition. Heating rate $\beta = 0.15$ K/min and same modulation as in (a). (c) $c_p^{\infty}(T)$ specific heat capacity after total relaxation (result of relaxation-fit).

expansion coefficients evaluated from our modulated DSC data with those given in literature. The expansion of the free energy density $f(T, P)$ in terms of the temperature T and the polarisation P can be written as [20]

$$f(T, P) = f_0 + \frac{1}{2}A(T)P^2 + \frac{1}{4}\xi P^4 + \frac{1}{6}\zeta P^6 \quad (1)$$

where $A(T)$ follows a Curie–Weiss law $A(T) = (T - T_c)/C$ and the Curie constant C was shown [19] to be given by $C = 3\,560\,\mathrm{K}\varepsilon_0$. For a transition of second order ξ and ζ are positive.

As a consequence we obtain the dielectric equation of state

$$E(T, P) = \frac{\partial f}{\partial P} = A(T)P + \xi P^3 + \zeta P^5 \quad (2)$$

which results in the spontaneous polarisation

$$P_s^2(T) = P^2(T \leq T_c, E = 0) = \left\{-\xi + \sqrt{\xi^2 - 4A(T)\zeta}\right\}/2\zeta \quad (3)$$

From Eq. (1), we derive the entropy density $s(T,P)$

$$s(T, P) = -\frac{\partial f}{\partial T} = s_0(T) - \frac{1}{2C}P^2 \quad (4)$$

and the specific heat capacity

$$c(T) = \frac{T}{\rho}\frac{\partial s}{\partial T} = c_0(T) - \frac{T}{2\rho C}\frac{\partial (P^2)}{\partial T} \quad (5)$$

where f_0, s_0 and c_0 denote the non-critical respective background (lattice) quantities and $\rho(328\,\mathrm{K}) = 1.6574\mathrm{g/cm}^2$ [23] the mass density. We stress, that according to Eqs. (4) and (5) both quantities s and c are simply determined by P^2 or its derivative $\partial(P^2)/\partial T$, respectively, both of which are typical for the process under consideration. If the process is realised in a way that $P = 0$, both entropy and specific heat capacity are given by their respective background values. If, on the other hand, the condition $E = 0$ is realised, Eq. (3) holds and both quantities are determined by the behaviour of the spontaneous polarisation P_s. Accordingly, we obtain for the anomalous contribution to the specific heat capacity $\Delta c = c - c_0$ for the case $E = 0$

$$(T/\Delta c)^2 = (2\rho C^2)^2(\xi^2 - 4A(T)\zeta) \quad (6)$$

This relation realises a linear temperature dependence for $(T/\Delta c)^2$, which renders possible the determination of the constants ξ and ζ of the potential, if C is known.

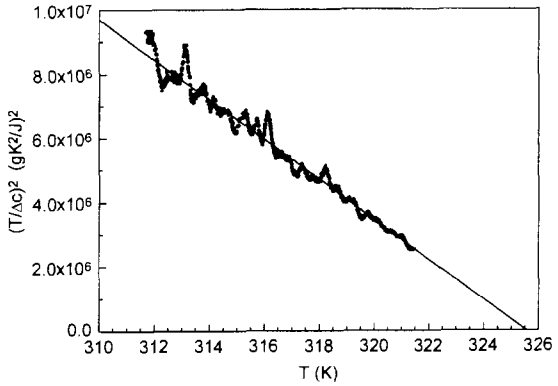

Fig. 6. Plot of $(T/\Delta c_{E=0})^2$ as a function of T. Straight line – linear fit; Intersection with T-axis at 325.51 K.

The excess specific heat was estimated by taking in Fig. 5(a) the difference between the measured value for C_p and the one extrapolated from the region $T>T_c$ yielding a transition entropy $\Delta S = 1.31 \times 10^{-2}\,\mathrm{Jg^{-1}\,K^{-1}}$. This value is similar to values published by Strukov [24] and Tello [25] ($1.42 \times 10^{-2}\,\mathrm{Jg^{-1}\,K^{-1}}$ and $1.38 \times 10^{-2}\,\mathrm{Jg^{-1}\,K^{-1}}$ respectively).

Using Eq. (6) we evaluated from our data (Fig. 6) the expansion parameters of the Landau potential $\xi = 4.6 \times 10^{11}\mathrm{Vm^5/C^3}$ and $\zeta = 4.5 \times 10^{14}\mathrm{Vm^9/C^5}$. The rather good agreement with literature data [26] yielding $\xi = 6.25 \times 10^{11}\mathrm{Vm^5/C^3}$ and $\zeta = 4.02 \times 10^{14}\mathrm{Vm^9/C^5}$ confirm again the efficiency of the modulated DSC technique for the investigation of structural phase transitions.

A further great advantage of the modulated DSC technique results from its ability to perform quasi-isothermal measurements in the time domain (TDM-DSC technique). This gives the opportunity to study the evolution of slow kinetic effects in the vicinity of phase transitions, such as domain movements, diffusion of impurities, depolarisation effects, etc. We have used this technique to qualitatively study the effect of floating boundary conditions of TGS on its caloric properties. For this purpose, we used a piece of as-grown TGS single crystal which we have cleaved along the (010) cleavage plane. Without any pre-treatment, this crystal piece was put into an ordinary aluminium pan.

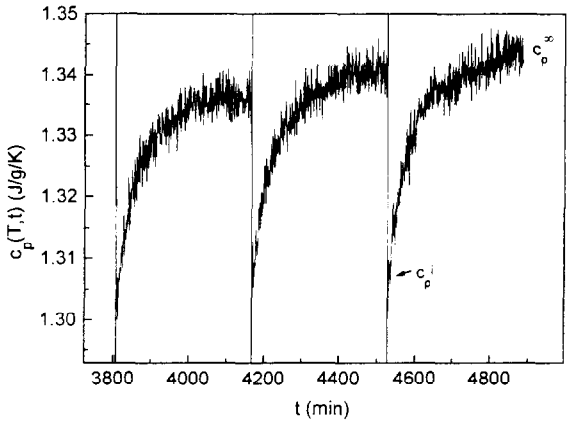

Fig. 7. Quasi-isothermal TDM-DSC on TGS without specified boundary conditions; $c_p(T,t)$ for temperatures 320.40, 320.64, and 320.90 K showing very slow relaxations in the time domain ($A_T = 0.2\,K$, $P_m = 60\,s$).

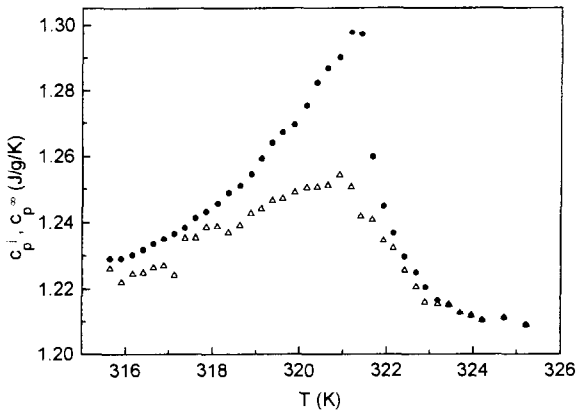

Fig. 8. Instantaneous (c_p^i, •) and relaxed values (c_p^∞, Δ) of the specific heat capacity of TGS measured after temperature steps of $\Delta T \approx 0.25\,K$.

The modulated DSC measurements have been performed in three steps (Fig. 5). Close to T_c, we have used the TDM-DSC technique (Fig. 5, curve c) in order to resolve c_p-relaxations appearing just below T_c. Within the non-relaxing temperature regimes $T \ll T_c$ (Fig. 5, curve b) and $T > T_c$ (Fig. 5, curve d), we used modulated DSC in the continuous heating mode ($\beta = 0.15\,K/min$, $P_m = 60s$ and $A_T = 0.2\,K$). Fig. 7 shows some representative c_p-relaxations in the time domain. The average relaxation time of this process increases on approaching T_c from below and ends definitely at T_c.

We emphasise that the c_p-relaxation processes *do not* connect subsequent values of dynamic equilibrium, but start at each new relaxation step below the relaxed value of the previous relaxation step. However, according to Fig. 8 the initial specific heat values measured immediately after a new temperature step (j), $c_p^i(T_j)$, exceeds the back-ground specific heat of the crystal lattice. Moreover, the relaxed specific heat values $c_p^\infty(T_j)$ at floating boundary conditions do not reach the appropriate values of the samples measured at $E = 0$.

Obviously, in as much the order parameter P_s causes the excess specific heat peak at the phase transition of TGS the modulated DSC method is sensitive to the variations of the order parameter. For the boundary condition $E = 0$, the variation of $P = P_s$ reaches the maximum value. If we abandon this condition, the resulting variation of P will become smaller, thereby yielding smaller values of heat capacity, i.e. $c_p < c_{p,E=0}$ (Fig. 5(a) and (c)).

The observations of the $c_p(T, t)$ results measured with TDM-DSC can be summarised as follows:

1. Starting at a temperature T and the corresponding equilibrium value $c_p^\infty(T)$ of the heat capacity, a temperature step of $\Delta T \approx 0.25\,K$ always reveal an instantaneous decrease of the heat capacity:
$$c_p^i(T + 0.25\,K) < c_p^\infty(T)$$
2. As a function of time, the heat capacity of TGS increases starting at c_p^i and reaches an equilibrium value c_p^∞. As a function of temperature, the relaxed heat capacities follow the relation:
$$c_p^\infty(T + 0.25\,K) > c_p^\infty(T)$$
3. On approaching the phase transition, the values of the resulting $c_p^i(T)$ and $c_p^\infty(T)$ curves increase (Fig. 8) being smoother for $c_p^i(T)$. The relaxation amplitude expressed by the difference $c_p^\infty(T) - c_p^i(T)$ also shows a pronounced increase (Fig. 9).
4. The characteristic relaxation time of the c_p relaxations, indicated by the increasing time interval necessary to record $c_p(t)$, also seems to increase.
5. At temperatures above T_c, no more relaxation of the heat capacity is observed.

The results of the TDM-DSC experiments lead us to the following preliminary interpretations: When in the ferroelectric phase, an increase of the temperature causes a decrease in electric polarisation. As a con-

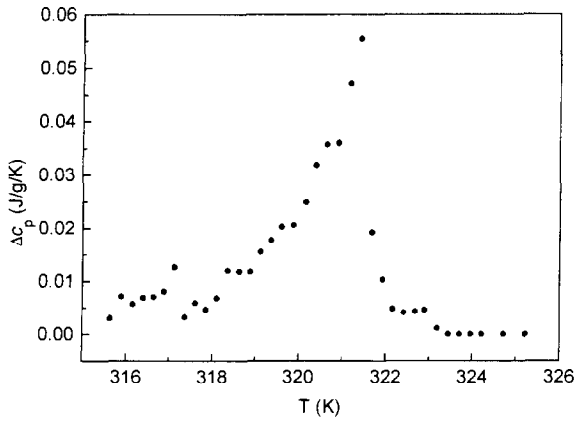

Fig. 9. Difference $\Delta c_p = c_p^{\infty} - c_p^{i}$ as a function of temperature.

sequence, there are surface charges on the sample. As the plate-like TGS sample is mounted in a standard aluminium pan, whose surfaces consist of aluminium oxide having a bad electrical conductivity, the surface charges cannot be removed immediately. Changing abruptly the temperature of this partially isolated electrical sample yields the initial boundary condition $D \approx P \approx$ const., where D is the magnitude of the electric displacement vector. $P =$ const. would yield the background specific heat of the crystal lattice. Looking upon the TGS sample in its aluminium pan as a capacitor–resistor parallel connection with an unknown ohmic resistance R, this parallel connection has a relaxation time $\tau_{C_p} = RC_p$. The capacitor C_p can only be discharged by a current via the resistor R, represented mainly by the finite conductivity of the sample surface, thus yielding the observed relaxing specific heat response. The deviation of $c_p^i(T)$ from the lattice background is probably due to the effect of ferroelectric domains. The planned quantitative treatment also must take into account the modulation effect itself.

Acknowledgements

This work was kindly supported by the Deutsche Forschungsgemeinschaft. All crystal material was kindly provided by Drs. J. Albers and A. Klöpperpieper.

References

[1] W. Hemminger and G. Höhne, Grundlagen der Kalorimetrie, Verlag Chemie, Weinheim, 1979.
[2] B. Wunderlich, Thermal Analysis, Academic Press, Harcourt Brace Jovanovich Publishers, Boston, MA (1990).
[3] M. Reading, B.K. Hahn and G.S. Crowe, US Patent 5,224,775, July 6 (1993).
[4] M. Reading, D. Elliot and V.L. Hill, J. Thermal Analysis, 40 (1993) 931.
[5] P.S. Gill, S.R. Sauerbrunn and M. Reading, J. Thermal Analysis, 40 (1993) 949.
[6] B. Wunderlich, Y. Jin and A. Boller, Thermochim. Acta, 238 (1994) 277.
[7] A. Boller, Y. Jin and B. Wunderlich, J. of Thermal Analysis, 42 (1994) 307.
[8] J.K. Krüger, K.-P. Bohn, R. Jiménez and Z. Schreiber, Colloid Polym. Sci., 274 (1996) 490.
[9] J.K. Krüger, K.-P. Bohn and R. Jiménez, Condensed Matter News, 5 (1996) 10.
[10] H. Iwasaki, S. Miyazawa, H. Koizumi, K. Sugii and N. Niizeki, J. Appl. Phys., 43 (1972) 4907.
[11] S. Nanamatsu, H. Sugiyama, K. Doi and Y. Kondo, J. Phys. Soc. Japan, 31 (1971) 616.
[12] T. Yamada, H. Iwasaki and N. Niizeki, J. Appl. Phys., 43 (1972) 771.
[13] A. Klöpperpieper, H.J. Rother, J. Albers and K.H. Ehses, Ferroelectrics Letters, 44 (1982) 115.
[14] U. Schell, Ferroelectrics Letters, 4 (1985) 123.
[15] K.-P. Frühauf, E. Sauerland, J. Helwig and H.E. Müser, Ferroelectrics, 54 (1984) 293.
[16] S.A. Taraskin, B.A. Strukov and V.A. Meleshina, Sov. Phys. – Solid State, 12 (1970) 1089.
[17] S. Hoshino, T. Mitsui, F. Jona and R. Pepinsky, Phys. Rev., 107 (1957) 1255.
[18] S. Triebwasser, I.B.M. J. Research Development, 2 (1958) 212.
[19] J.A. Gonzalo, Phys. Rev., 144 (1966) 662.
[20] J. Grindlay, An Introduction to the Phenomenological Theory of Ferroelectricity, Pergamon Press, Oxford (1970).
[21] B.A. Strukov, T.P. Spiridonov, K.A. Minaeva, V.A. Fedorikhin and A.V. Davtyan, Sov. Phys. Crystallogr., 27 (1982) 190.
[22] S.A. Taraskin, B.A. Strukov, V.A. Fedorikhin, N.V. Belugina and V.A. Meleshina, Sov. Phys. – Solid State, 19 (1978) 1721.
[23] N.D. Gavrilova, V.K. Novik and P.S. Smirnov, Sov. Phys. – Solid State, 19 (1977) 2147.
[24] B.A. Strukov, Sov. Phys. – Solid State, 6 (1964) 2278.
[25] M.J. Tello and J.A. Gonzalo, Proceedings of 2nd Internat. Meeting on Ferroelectrics, J. Phys. Soc. Japan, 28 (1970) 199.
[26] H.M. Choe, J.H. Judy and A. van der Ziel, Ferroelectrics, 15 (1977) 181.